Uniaxial magnetic anisotropies in Fe films on single crystal and virtual Ge(001) substrates studied with spin polarized inverse photoemission and MOKE

M. Cantoni, M. Riva, R. Bertacco, and F. Ciccacci

L-NESS, Dipartimento di Fisica del Politecnico di Milano, Via Anzani 42, 22100 Como, Italy
(Received 12 April 2006; revised manuscript received 11 July 2006; published 19 October 2006)

Fe films have been grown at room temperature on standard Ge(001) single crystals and virtual Ge/Si$_{1-x}$Ge$_x$/Si(001) substrates, and their magnetic properties extensively investigated *in situ* by spin polarized inverse photoemission and magneto-optical Kerr effect. Two different uniaxial anisotropies have been found to coexist. The first one, giving rise to a [110] easy axis, is associated to the Fe/Ge interface: it disappears at large thickness (more than 10 Fe layers), while dominates in very thin films (5 Fe layers) on virtual substrates. A second anisotropy, considerably smaller in strength, originates a [010] or [100] easy axis: it persists at large thickness (up to 60 Fe layers) and is essentially associated to bulk properties. However, this is not an intrinsic property, being related to the sample preparation conditions, i.e., substrate sputtering at oblique incidence for cleaning and Fe deposition at oblique incidence. The uniaxial easy axis is always perpendicular to the incidence plane, either of the Fe atoms flux or the ion beam, with a larger effect of deposition conditions with respect to sputtering. Our results give evidence of a strong correlation between morphology and magnetism in Fe/Ge/Si$_{1-x}$Ge$_x$/Si(001) and Fe/Ge(001) films, opening the way to the engineering of magnetic properties via the control of the preparation conditions.

I. INTRODUCTION

Due to the growing interest in magnetic multilayers, in the last decade the magnetic properties of thin and ultrathin films have been widely studied with great attention to their peculiarities with respect to bulk materials.[1,2] The reduction of film thickness gives evidence that surface and interface contributions strongly influence the magnetic anisotropy, while the loss of translational invariance perpendicular to the surface and the reduction of in-plane symmetry, due for example to defects or periodic ripples, may introduce new magnetic anisotropy terms. In particular, the correlation between morphology and magnetism has been investigated, and the opportunity of using nanostructures to induce "controlled" anisotropies in thin films clearly demonstrated.[3,4]

A relevant feature of epitaxial magnetic thin films is the evolution via irreversible jumps of the in-plane magnetic configuration, showing abrupt changes at well-defined applied magnetic field strengths. Each step corresponds to a transition between two single-domain configurations and the energetic of domain formation and propagation is crucial for a complete understanding of magnetization processes. The low dipolar energy, reduced symmetry, and well-defined anisotropies typical of thin films allow for a reduction of the problem complexity, so that relatively simple models can be applied.[5]

The case of Fe thin films on Ge(001) is particularly interesting due to the high quality of this interface and its potential application for spin injection in semiconductors. Room-temperature growth is epitaxial and without sizeable intermixing, and films thicker than 20 Å present structural and electronic properties typical of single crystal bcc Fe.[6] In comparison with other ferromagnet/semiconductor epitaxial interfaces, Fe/Ge(001) shows higher surface order, an electronic structure very similar to that of Fe(001) and the lowest thickness at which ferromagnetism appears (4.3 Å).[7] Finally,

the growth of high quality Fe films on so-called "virtual" Ge/Si$_{1-x}$Ge$_x$/Si(001) substrates,[8] instead of usual single crystal Ge(001) substrates, is very attractive because it offers new opportunities for integration of magnetic thin films with existing conventional Si-based electronics.[6]

In this paper, we extensively discuss the magnetic anisotropies of Fe films grown on single crystal and virtual Ge(001) substrates. The existence of an uniaxial anisotropy in Fe/Ge(001), with easy axis along the [110] direction of the Fe lattice, is well known.[9,10] Here we focus on additional anisotropies, induced either by the substrate or by the preparation procedures, as seen by *in situ* magneto-optical Kerr effect (MOKE) and spin polarized inverse photoemission (SPIPE). We present a detailed study of the Fe films magnetic properties by varying different parameters, namely: (i) Fe film thicknesses, from 5 to 60 equivalent monolayers (ML, 1 ML corresponds to 1.43 Å, the layer spacing of bcc Fe); (ii) substrate, either single crystal Ge(001) or virtual Ge/Si$_{1-x}$Ge$_x$/Si(001); (iii) sample preparation conditions, i.e., substrate cleaning by ion sputtering and Fe deposition. Our results indicate that for thicknesses below 15 ML two different uniaxial anisotropies coexist, giving rise to [110] and [010] easy axes. Data are interpreted by an appositely developed phenomenological model. Relations between different uniaxial anisotropies and synthesis parameters are also discussed, in view of magnetic properties engineering (easy axes direction and anisotropy strength) in Fe thin films on Ge(001) and Ge/Si$_{1-x}$Ge$_x$/Si(001) substrates for spin electronics applications.[11]

II. EXPERIMENT

The Ge/Si$_{1-x}$Ge$_x$/Si(001) virtual substrate was prepared by low-energy plasma-enhanced chemical vapor deposition (LEPECVD)[12] in the same way described in Ref. 6. Starting

from a Si(001) substrate, subsequent layers of a $Si_{1-x}Ge_x$ alloy are grown, with x linearly increasing from $x=0$ to $x=1$ (pure Ge) over a thickness of 10 μm. On top of the graded buffer layer, a 1 μm layer of pure Ge was grown in order to achieve complete strain relaxation.

Commercial Ge wafers were used for standard single crystal substrates. Both types of substrates underwent exactly the same preparation and surface cleaning procedures: chemical cleaning, and subsequent insertion via an interlock chamber into the ultrahigh vacuum (UHV, $p < 1 \times 10^{-10}$ torr) system,[13] where several sputtering-annealing cycles produced clean surfaces (as checked by x-ray photoemission spectroscopy) with a sharp (2×1) low-energy electron diffraction pattern. (see Ref. 6 for details).

Fe films were grown in UHV with the substrate at room temperature, in order to reduce interdiffusion between Fe and Ge,[9] by molecular beam epitaxy (MBE) at a rate of $\sim$1.3 Å/min, as monitored by a calibrated quartz microbalance. Films in the 5–60 ML range have been studied; the uncertainty in the deposited film thickness is estimated to be within ±10%. The Fe lattice parameter being roughly half that of Ge, epitaxial growth takes place with the Fe [100] direction parallel to Ge [100] direction.

The films were studied *in situ* by MOKE and SPIPE at room temperature. MOKE loops are taken by applying the external magnetic field (H) along either the [100] or the [010] crystallographic axis of the Fe lattice, and collecting the signal in both transverse and longitudinal mode.[14] SPIPE measurements are performed in the isochromat mode and in remanence, after having magnetized the sample with an in-plane pulsed magnetic field of 2000 Oe, applied along either the [100] or the [010] axis, as described in detail elsewhere.[15] SPIPE is a spectroscopic tool mainly employed for investigating the spin resolved electronic structure of unoccupied states. It can effectively be used, however, also for studying magnetic anisotropies, by providing the orientation of the remanent magnetization (M_0) after application of a given H. This method is particularly useful in thin films since, in case of a strong uniaxial anisotropy, it gives immediately the orientation of the easy axis, coincident with M_0. In our apparatus the incident electron beam polarization (P) is parallel to the sample surface and continuously reverted, so that it assumes two opposite values $P[\sigma^+]$ ($P[\sigma^-]$) depending on the polarization (σ) of the circularly polarized light incident on the GaAs photocathode. $P[\sigma^+]$ ($P[\sigma^-]$) are fixed in space while the sample can rotate in front of the electron beam in order to change the angles between P, the crystallographic axes and M_0. Due to shape anisotropy the magnetization lies in-plane for films of Fe/Ge,[16] and in the present investigation H is applied either along [100] or [010], so all the three vectors (H, M and P) lie in plane. We then define ϕ, θ, and α as the angles between the [100] direction of the Fe lattice and the vectors H, M, and $P[\sigma^+]$, respectively [see Fig. 1(a)]. The asymmetry between σ^+ and σ^- channels in SPIPE spectra is proportional to the scalar product $P \cdot M_0$,[17] so that its maximum corresponds to P being parallel or antiparallel to M_0, i.e., $\alpha - \theta_0 = 0°$ or 180°, where θ_0 is the angle between M_0 and the [100] direction. In our setup, when a majority peak appears in the σ^+ (σ^-) channel, M_0 and $P[\sigma^+]$ are an-
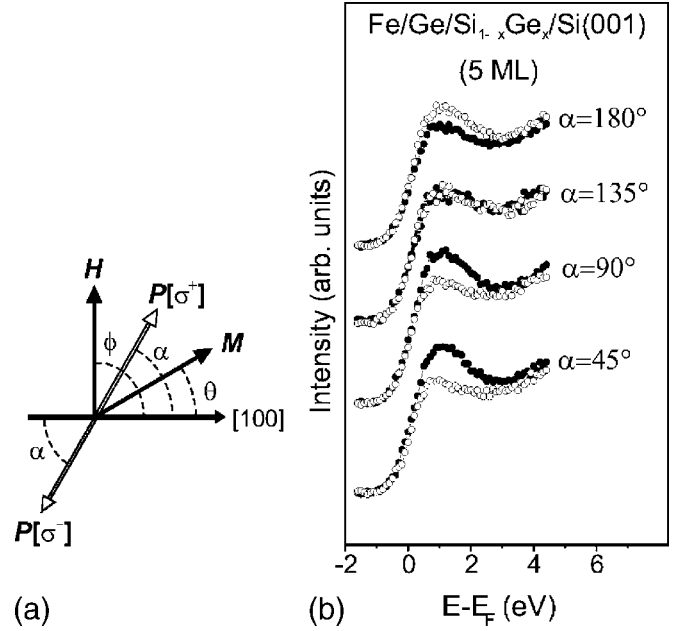

FIG. 1. (a) The reference frame for H, M, and P supposed in plane. (b) The spin polarized inverse photoemission spectra at different angles α on 5 ML of Fe/Ge/$Si_{1-x}Ge_x$/Si(001), with H applied along [100]; full and empty dots refer to different directions of the incident electron spin; for the case of 45° full dots correspond to minority-spin electrons.

tiparallel (parallel), whereas M_0 and $P[\sigma^-]$ are parallel (antiparallel). By rotating the sample in front of the electron beam, it is then possible to find the configuration which maximize the spin asymmetry and find the full orientation of M_0.

To clarify this method we present the application to the case of 5 ML of Fe grown on a virtual substrate Ge/$Si_{1-x}Ge_x$/Si(001). The four SPIPE spectra of Fig. 1(b) have been collected at $\alpha=180°$, 135°, 90°, and 45° ($P[\sigma^+]$ is directed, respectively, along [$\bar{1}$00], [$\bar{1}$10], [010], and [110] after application of H along the [100] direction ($\phi=0$). As it is well known for thin Fe(001) films,[18] the well-defined peak at $\sim$1 eV above the Fermi level has a minority spin character. In Fig. 1(b) the spectral asymmetry is null at $\alpha=135°$ and maximum at $\alpha=45°$, but in the latter case the minority peak appears in the σ^+ channel (filled circles).[6,7] In this particular case M_0 is parallel to $P[\sigma^+]$ and directed along the [110] axis ($\theta_0=45°$). At variance with thick epitaxial films, the remanent magnetization is not parallel to the applied magnetic field, thus indicating the presence of relevant uniaxial anisotropies.

Combining *in situ* MOKE and SPIPE allows us to investigate and clarify the origin of the three different magnetic anisotropy terms that coexist in Fe/Ge(001) films. The case of single crystal substrates will be presented at first, in order to discuss the effect of "intrinsic" sources only, without any additional complication due to virtual substrate morphology. Finally the more complex behavior of Fe/Ge/$Si_{1-x}Ge_x$/Si(001) films in the whole range 5–60 ML will be discussed.
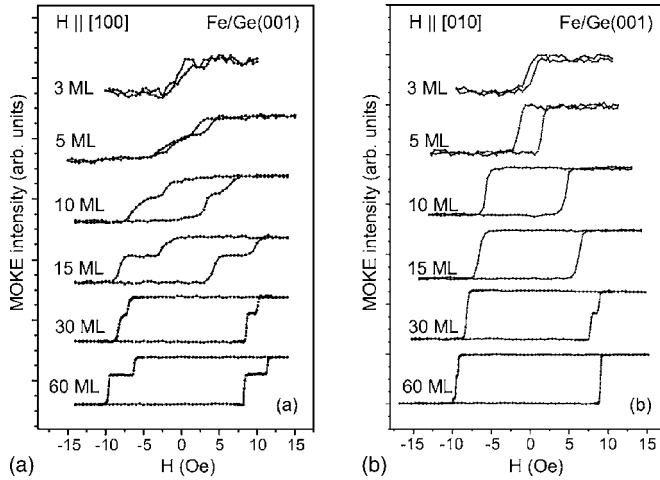
FIG. 2. MOKE loops on Fe/Ge(001) films of different thicknesses: (a) longitudinal loops, with **H** applied along the [100] direction; (b) transverse loops, with **H** applied along the [010] direction.

III. SINGLE CRYSTAL SUBSTRATES

A. SPIPE and MOKE results

Figure 2 reports MOKE hysteresis loops, recorded *in situ* with **H** directed along [100] and [010] (in longitudinal and transverse configurations, respectively), from Fe films with thickness from 3 to 60 ML grown on the single crystal Ge(001). Strong variations are seen when changing the applied field direction, clearly indicating the breaking of cubic symmetry. The stepped shape of longitudinal loops in the range 15–60 ML, together with the absence of significant steps in the square transverse loops, immediately suggests the presence of a uniaxial anisotropy term with easy axis along the [010] direction.[19] The persistence of this behavior even at a large thickness (60 ML) rules out a pure interfacial origin, indicating that this term is related to the growth mechanism, as better shown below. For 3, 5, and 10 ML films, instead, the longitudinal loop shapes are different from a simple stepped or square profile: they can be explained only by introducing a second uniaxial anisotropy term, with easy axis along the [110] direction of the Fe lattice. These MOKE data are in excellent agreement with the orientation of M_0 determined by SPIPE using the method outlined above, as schematically shown in Fig. 3(a). At low thickness (3–5 ML) the uniaxial anisotropy with [010] easy axis dominates, and M_0 is parallel to [010], even if **H** has been applied along the [100] direction, in perfect agreement with the longitudinal loop of Fig. 2(a), displaying no remanence at these thicknesses. The relative strength of such a term decreases with thickness, so that M_0 gradually approaches the direction of **H** and finally stays parallel to it above 15 ML. Correspondingly, the hysteresis loops of Fig. 2(a) display remanence.

B. Origin of (010) magnetic anisotropy

As discussed above, MOKE loops in Fig. 2 support the existence of a magnetic uniaxial anisotropy even in thick
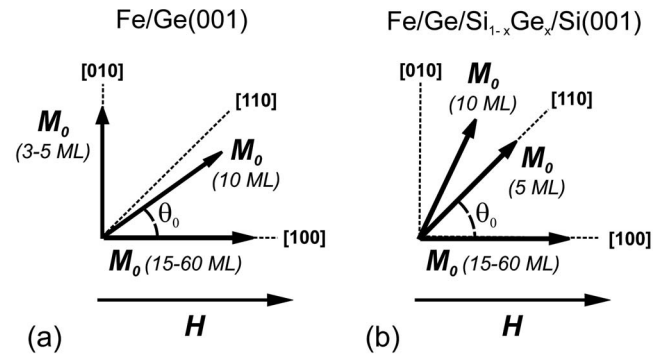

FIG. 3. Experimentally determined orientation of M_0 after application of **H** along [100] in Fe films with different thicknesses on (a) Ge(001) and (b) Ge/Si$_{1-x}$Ge$_x$/Si(001). The determination has been done by applying the SPIPE analysis as described in the text [cf. also Fig. 1(b)].

films (60 ML), with [010] easy axis. This is somehow an unexpected result for Fe films on semiconductors: typically the uniaxial easy axis in Fe/Ge(001),[9,10] Fe/GaAs(001),[20] and Fe/ZnSe(001)[21] has ⟨110⟩ orientation and originates from substrate or interface properties like the directionality of dangling bonds. Different possible sources of uniaxial anisotropy with [010] easy axis in Fe films on different substrates are reported in the literature. A first possibility is related to film deposition at oblique incidence, as in Fe/MgO(001)[22,23] and Co/Cu(001).[24] Actually, in our experimental setup, the incidence angle is 25° with respect to the normal, so that the observed anisotropy can be partially ascribed to such an effect. A second source of anisotropies is nanostructuration of Fe film induced by ion bombardment, as in Co/Cu(001).[3] Even though this does not directly apply to our case, since the films do not undergo any sputtering process after growth, some influence of the substrate sputtering can however be expected. In fact, our cleaning procedures of the Ge substrates typically involve Ar$^+$ ions sputtering at 1 keV and ~1 μA/cm^2, at 60° out from normal incidence. The influence of ion sputtering on the formation of strongly directional structures,[11] with dimensions ranging from few to hundreds nm, has indeed been reported.[25] To our knowledge, however, no effect of substrate sputtering on the magnetic anisotropy of a magnetic overlayer has been so far observed.

In order to gain a better comprehension of the influence of these mechanisms, ultrathin films grown onto a single crystal substrate without miscut are well suited. In fact spurious effects arising from the substrate morphology can be ruled out and the reduced thickness enhance interfacial contributions. A set of three Fe films with thickness of 5 ML were synthesized with different combinations of sputtering/deposition planes of incidence, as reported in Table I. The corresponding MOKE loops taken *in situ* are reported in Fig. 4.

We consider first films *A* and *C*, grown with the same incidence plane for both sputtering and MBE: (010) and (100) for *A* and *C*, respectively. In film *A*, if **H** is applied along the [100] direction (full dots), a stepped loop is detected, while if **H** is applied along the [010] one (empty dots) the loop is essentially square: this suggests the existence of a strong uniaxial anisotropy with [010] easy axis, i.e., perpen-

TABLE I. Sputtering/deposition conditions for Fe/Ge(001) films with thickness of 5 ML.

Film	Incidence plane	
	Sputtering	Deposition
A	(010)	(010)
B	(100)	(010)
C	(100)	(100)

dicular to the incidence plane of sputtering/deposition. SPIPE confirms this scenario: Figure 5(a) reports SPIPE spectra collected from film A at $\alpha=180°$ and $90°$ ($P[\sigma^+]$ is directed, respectively, along $[\bar{1}00]$ and $[010]$), with H applied along the $[100]$ direction. Following the interpretation scheme of Fig. 1, the spectral asymmetry is maximum at $\alpha=90°$ and the minority peak appears in the σ^+ channel (filled circles), then M_0 is parallel to $P[\sigma^+]$ and directed along the $[010]$ axis ($\theta_0=90°$). The same result holds true also with H along $[010]$ (not shown). Film C presents exactly the same loop shapes of film A but longitudinal and transverse loops are completely exchanged, indicating that now the uniaxial easy axis is along the $[100]$ direction. Accordingly SPIPE reveals that M_0 has a $[100]$ orientation after application of H along either $[100]$ (see Fig. 5(b): the spectral asymmetry is maximum at $\alpha=180°$ and the minority peak appears in the
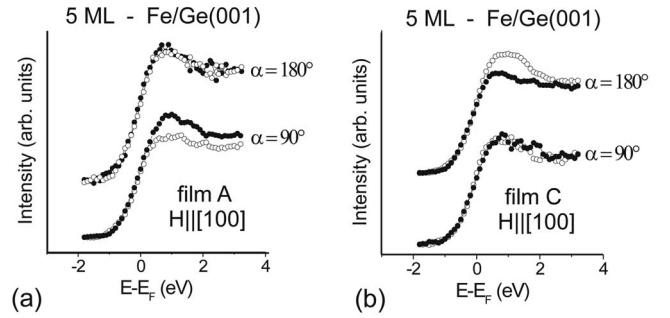
FIG. 5. Spin polarized inverse photoemission spectra at different angles α on 5 ML of Fe/Ge(001), with H applied along $[100]$. The sputtering/MBE planes of incidence are: (a) (010)/(010); (b) (100)/(100).

σ^- channel (empty circles), then M_0 is parallel to $P[\sigma^-]$ and θ_0 is $0°$) or $[010]$ (not shown). We can then conclude that, if sputtering and deposition are performed with the same incidence plane, the direction of the uniaxial easy axis is always perpendicular to this plane. This is not surprising because sputtering at oblique incidence may lead to the formation of periodic ripples, with wave vector parallel to the ion beam direction and wavelength of the order of 200 nm:[25] if, for example, the ion beam is incident along the plane (010), as in film A, the wave vector is parallel to $[100]$ and peaks and troughs are elongated in the $[010]$ direction. This kind of morphological anisotropy is similar to that induced by terraced or vicinal substrates: the substrate fourfold symmetry is broken in both cases, and a magnetic uniaxial anisotropy develops in the overlayer.[26,27] Film deposition at oblique incidence is expected to produce similar periodic structures with the wave vector parallel to the incidence plane. In the case of Fe/MgO(001), for example, a uniaxial easy axis develops in the direction parallel to the elongation of peaks and troughs, i.e., perpendicular to the deposition incidence plane.[23] By analogy, if the Fe flux is incident along the (010) plane, as in film A, a $[010]$ easy axis is then expected, in agreement with our findings. Both sputtering and film deposition produce a periodic structure with peaks and troughs elongated in direction perpendicular to the incidence plane, which coincides with the orientation of the uniaxial anisotropy easy axis.

For film B the sputtering and deposition incidence planes are different, (100) and (010) respectively. MOKE loops in Fig. 4(b) bear much resemblance to those of film A, with a decrease of the coercive field in the transverse loop; the orientation of M_0 determined by SPIPE is also the same as for case A. The uniaxial anisotropy is then mainly determined by film deposition out from normal incidence, while the effect of sputtering appears as a reduction of the coercive field. This is not surprising, since after sputtering the substrates undergo a reordering annealing procedure which is expected to reduce any possible corrugation induced by ion bombardment, so that the latter acts only as a perturbation.

To summarize this section, we have demonstrated that in Fe/Ge(001) films the uniaxial anisotropy with $[010]$ (or $[100]$) easy axis, persisting even in thick films (60 ML), can be ascribed to sample preparation conditions, and mainly to film deposition at oblique incidence.
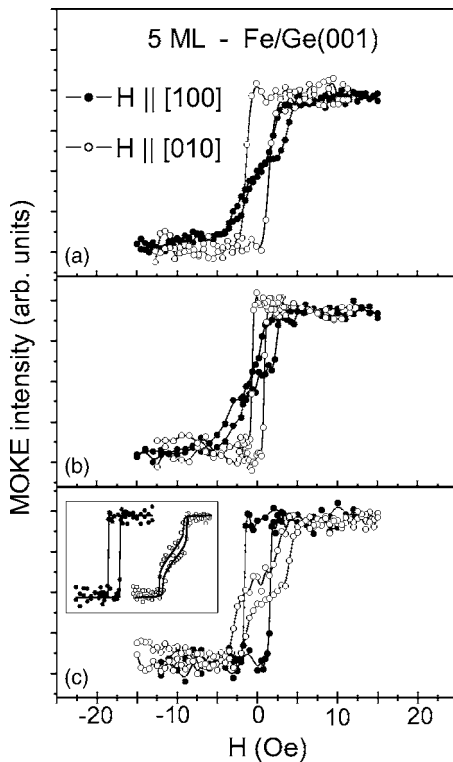

FIG. 4. MOKE loops on 5 ML of Fe/Ge(001); the sputtering/MBE planes of incidence are: (a) (010)/(010); (b) (100)/(010); (c) (100)/(100). Filled (empty) dots refer to longitudinal (transverse) configuration. In the inset the measured (circles) and simulated (continuous lines) hysteresis loops from film C are reported.
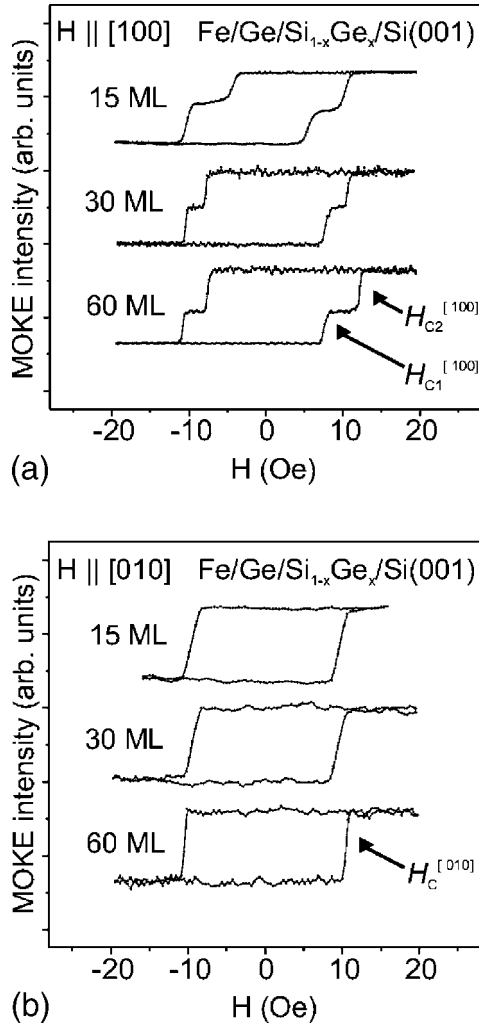
FIG. 6. MOKE loops on $Fe/Ge/Si_{1-x}Ge_x/Si(001)$ films of different thicknesses: (a) longitudinal loops; (b) transverse loops.

IV. VIRTUAL SUBSTRATES

Figure 3(b) shows the orientation of the remanent magnetization M_0 determined by SPIPE, after application of H along [100], in Fe films with thickness ranging from 5 [see Fig. 1(b)] to 60 ML grown on virtual $Ge/Si_{1-x}Ge_x/Si(001)$ substrates. The comparison with films grown on single crystal substrates, shown in Fig. 3(a), clearly shows that the situation is similar except for 5 ML: in this case M_0 is directed along the [110] direction, thus indicating that the uniaxial anisotropy with [110] easy axis is more relevant for virtual substrates. The picture arising from SPIPE essentially shows that virtual substrates give rise to a very peculiar magnetic behavior at low coverage, while above 15 ML they behave very much the same as single crystal ones. Similar findings are also obtained by MOKE data: we reported in Fig. 6 the case for 15–60 ML thick films, while ultrathin films will be considered in a later section. The MOKE loops have been recorded *in situ* with H directed along [010] and [100] (transverse and longitudinal configuration, respectively). Fe films are synthesized with the same preparation conditions (sputtering/deposition incidence planes) of film A on

Ge(001) described in the previous section. As for Fe/Ge(001) in the same thickness range (Fig. 2), longitudinal loops are stepped while transverse loops are square, indicating the presence of an uniaxial anisotropy with easy axis along [010]. In consideration of the interest of $Fe/Ge/Si_{1-x}Ge_x/Si(001)$ films in view of possible integration of epitaxial magnetic structures on Si, in the following we present a detailed analysis of the anisotropy evolution based on MOKE data taken on such films. Due to the above similarity with single crystals substrates, however, such discussion holds true for the last case too (apart from ultrathin films). Such an analysis is based on an appositely developed phenomenological model described below.

A. Phenomenological model of the magnetization process

For a better comprehension of magnetism in Fe thin films on Ge(001) and $Ge/Si_{1-x}Ge_x/Si(001)$, a simple phenomenological model including different anisotropy terms has been developed, and the film magnetic properties have been extracted by fitting the measured hysteresis loops. Second-order effects, as dynamics of domain walls propagation and Barkhausen noise,[28] are neglected, while the magnetization M is supposed to lie in plane. The total energy (E) of an arbitrary single domain configuration can be written as[29]

$$E = \frac{K_1}{4}\sin^2 2\theta + K_u^{[010]}\sin^2(\theta - \pi/2) + K_u^{[110]}\sin^2(\theta - \pi/4)$$
$$- MH\cos(\theta - \phi), \tag{1}$$

where ϕ and θ are the angles between the direction [100] of the Fe lattice and the vectors H and M, respectively, as shown in Fig. 1(a). The intensity of M coincides with the Fe saturation value, that is $M_S = 1.719 \times 10^6$ A/m,[28] while the angle θ determines the effective projection seen by MOKE. Three different in-plane anisotropy terms are taken into account, a cubic one (K_1) and two uniaxial ($K_u^{[010]}$ and $K_u^{[110]}$). K_1 is the effective cubic anisotropy constant: in films thicker than 10 ML its value is assumed, to a first approximation, to be independent from the film thickness and equal to the bulk Fe(001) value (4.8×10^4 J/m³).[28] In thinner films, however, it can be significantly lower because of an interfacial contribution with the opposite sign.[30] $K_u^{[010]}$ and $K_u^{[110]}$ are the uniaxial anisotropy constants associated to the [010] and [110] easy axes, respectively. In the Stoner-Wohlfarth model of magnetization proceeding via coherent rotation, for a given value (H) and direction (ϕ) of the applied field H, the resulting magnetization orientation (θ) corresponds to a local minimum of $E(\theta)$. According to Cowburn et al.,[19] however, in thin epitaxial films the transition between single domain states, corresponding to local minima of $E(\theta)$, can also result from the sweeping of a small number of domain walls across the surface. The involved activation energy can be neglected since this will happen at defects and film inhomogeneities, and does not represent a limiting factor. The critical parameter is instead the energy needed to unpin the walls, so that they can propagate freely across the sample. In this simple scheme, a phenomenological constant ε is introduced, which represents the maximum height of the defect energy barrier

that the domain walls encounter as they propagate. In order to change the magnetization direction, the energy gain of the transition must be greater or equal to the energy cost in overcoming the barrier. The physical basis of the model introduced by Cowburn *et al.* is the observation of sharp magnetization transitions at coercive fields much lower than the magnetic field needed to flatten the valley of the total energy and produce magnetization jumps via coherent rotation. This is exactly what we observe in Fig. 2, where the coercive fields for relatively thick films are of the order of 10 Oe, much less than the cubic anisotropy ($K_1 = 275$ Oe). Note that in this model no assumption has been made about the macroscopic nature of the pinning. In this sense ε is just a phenomenological parameter, whose connection with the macroscopic film properties is at this level indeterminate.

Neglecting coherent rotation, the form of the total energy (1) suggests that local minima of $E(\theta)$ can be found in the set $\{\theta = 0°, 45°, 90°, 180°, 225°, 270°\}$, and the "jumps" between two minima occur via nucleation of domains rotated by 45°, 90°, 135°, and 180° with respect to the original direction. However, the inspection of our loop shapes shows the absence of transitions associated to domain nucleation at 45° and 135°, because no steps corresponding to such rotations are detected. For this reason, only propagation of domains at 90° and 180°, with the associated energy barriers ε_{90} and ε_{180}, will be considered in the following. The simple analytical treatment introduced in Ref. 19 allows us to fit the data and extract the anisotropy constants for 15–60 ML, but is not satisfactory in the case of thinner films whose hysteresis loops shape clearly indicates that coherent rotation cannot be neglected. In order to analyze these cases, a numerical code including coherent rotation and magnetization jumps via domain propagation has been especially developed. Starting from an initial configuration (θ_0, H_0) the magnetic field is varied to $H' = H_0 + \Delta H$ and the exact position of the four local minima θ_i ($i = 1, 2, 3, 4$), close to $\theta_0, \theta_0 + 90°, \theta_0 + 180°$, $\theta_0 + 270°$, respectively, is found. For each local minimum the code verifies if the energetic cost of domain walls propagation is lower than the total energy gain arising from a magnetization jump, i.e., if

$$\varepsilon_{90,180} < E(\theta_0) - E(\theta_i). \tag{2}$$

In case the inequality (2) is satisfied for a given θ_j, with $j \neq 1$, a magnetic jump is energetically favored and the new magnetization orientation is given by θ_j. Otherwise the magnetization undergoes the continuous rotation imposed by the external magnetic field variation, with a final orientation θ_1 arising from the displacement of the minimum initially occupied. In this way hysteresis loops can be simulated and the fitting of experimental data provides the values of K_1, $K_u^{[010]}$, $K_u^{[110]}$, ε_{90}, ε_{180}, which are treated as free parameters.

As a result, we find that the [110] anisotropy is not negligible only in thin films; instead, in thick films $K_u^{[110]}$ is much smaller than $K_u^{[010]}$, and the [110] term can be neglected.[31] Even though this definitely applies to thin films on virtual substrates, it is somehow true also for such films on single crystal substrates. For instance, considering the case of 5 ML Fe/Ge(001) films, whose loops are reported in

Fig. 4, the fitting procedure for film C [cf. Fig. 4(c)] gives rise to the following values of the cubic and uniaxial anisotropy constants: $K_u^{[110]} : K_u^{[100]} : K_1 = 1 : 2 : 2$. As expected, exactly the same values are obtained also for film A, where $K_u^{[100]}$ is replaced by $K_u^{[010]}$.

B. Discussion: thick films (15–60 ML)

The analysis is considerably simpler because the contribution of uniaxial anisotropy with [110] easy axis is rather small for thick films (15–60 ML) on virtual substrates,[32] while the situation for ultrathin (<15 ML) films is more complex, and will be discussed in a following section. As noted above, the results shown in Fig. 6 indicate the presence of an uniaxial anisotropy with easy axis along [010]. On the contrary, the surface/interface uniaxial anisotropy with [110] easy axis has a negligible contribution at these relatively large coverage,[9] and, as a matter of fact, hysteresis loops can be simulated assuming $K_u^{[110]} = 0$. The only uniaxial anisotropy term that survives in Eq. (1) is $K_u^{[010]}$ so that the total energy E can be written as

$$E = \frac{K_1}{4} \sin^2 2\theta + K_u^{[010]} \sin^2(\theta - \pi/2) - MH \cos(\theta - \phi). \tag{3}$$

For an external magnetic field applied along [100] or [010] ($\phi = 0°$ or 90°, respectively), M can attain, by nucleation of domains rotated by 90° or 180°, the four directions [100], [010], [$\bar{1}$00], and [0$\bar{1}$0] ($\theta = 0°$, 90°, 180°, and 270°, respectively). MOKE loops in Fig. 6 show abrupt magnetization jumps (apart from second-order effects that smoothen the edges) that cannot be attributed to coherent rotation as coercive fields are too small when compared to cubic anisotropy. The simple analytical treatment proposed by Cowburn *et al.*[19] can then be applied to this case, assuming that M points always towards one of the four directions mentioned above. When H is applied along the uniaxial easy axis [010] ($\phi = \pi/2$), as in Fig. 6(b), loops are square and magnetization jumps are associated to nucleation of domains at 180°. If the H component along [010] is continuously increased from negative to positive values, M jumps from [0$\bar{1}$0] ($\theta = -90°$) to [010] ($\theta = 90°$) when the following condition is satisfied:

$$\Delta E = E_{[0\bar{1}0]} - E_{[010]} = 2MH \geq \varepsilon_{180}. \tag{4}$$

The corresponding coercive field $H_C^{[010]}$ is

$$H_C^{[010]} = \frac{\varepsilon_{180}}{2M}. \tag{5}$$

On the contrary, if H is applied along the [100] uniaxial hard axis ($\phi = 0$), as in Fig. 6(a), loops are stepped, thus indicating a magnetization reversal in two steps, each corresponding to nucleation of domains at 90°. Following Ref. 19, the jumps of M, from [$\bar{1}$00] to [010] and then to [100], require that

$$\Delta E_1 = E_{[\bar{1}00]} - E_{[010]} = K_u^{[010]} + MH \geq \varepsilon_{90}, \tag{6a}$$

TABLE II. Coercive fields and magnetic parameters of Fe/Ge/Si$_{1-x}$Ge$_x$/Si(001) thin films, as a function of the Fe thickness in the range 15–60 ML.

Thickness [ML]	$H \parallel [010]$	$H \parallel [100]$		$\dfrac{K_1}{M}$ [Oe]	$\dfrac{K_u^{[010]}}{M}$ [Oe]	$\dfrac{\varepsilon_{90}}{M}$ [Oe]	$\dfrac{\varepsilon_{180}}{M}$ [Oe]	$\dfrac{K_u^{[010]}}{K_1}$
	$H_C^{[010]}$ [Oe]	$H_{C1}^{[100]}$ [Oe]	$H_{C2}^{[100]}$ [Oe]					
15	9.6	4.9	10.4		2.7	7.7	19.1	1.0%
30	9.4	7.7	10.5	275	1.4	9.1	18.8	0.5%
60	10.5	7.6	11.5		1.9	9.5	21.0	0.7%

$$\Delta E_2 = E_{[010]} - E_{[100]} = -K_u^{[010]} + MH \geqslant \varepsilon_{90}. \qquad (6b)$$

The corresponding coercive fields are

$$H_{C1}^{[100]} = \frac{\varepsilon_{90} - K_u^{[010]}}{M}, \qquad (7a)$$

$$H_{C2}^{[100]} = \frac{\varepsilon_{90} + K_u^{[010]}}{M}. \qquad (7b)$$

By using Eqs. (4)–(7) and measuring the three coercive fields $H_C^{[010]}$, $H_{C1}^{[100]}$, and $H_{C2}^{[100]}$, it is then possible to calculate the magnetic parameters of Fe films listed in Table II for Fe/Ge/Si$_{1-x}$Ge$_x$/Si(001) films with thickness ranging from 15 to 60 ML.

In this estimation K_1/M is taken to be 275 Oe as in bulk bcc Fe. We note, however, that the determination of the exact value is behind our experimental accuracy: $K_1/M > 100$ Oe for 30 and 60 ML and >50 Oe for 15 ML would produce the same loop shapes, so that each value in these ranges could be equivalently used. Nevertheless, this is not a crucial point for the following discussion, the main information being that the ratio $K_u^{[010]}/K_1$ is lower than 6% in any case, even assuming $K_1/M = 50$ Oe. This is a further confirmation that stepped loops measured with $H \parallel [100]$ cannot be explained in terms of coherent rotation because, in the latter case, $K_u^{[010]}$ should be of the same order of magnitude of K_1. It is also worthwhile to note that, during the intensity decrease of H down to zero in the [100] direction in Fig. 6(a), M does not undergo any transition: M_0 is directed along [100] and parallel to H, as shown by SPIPE.
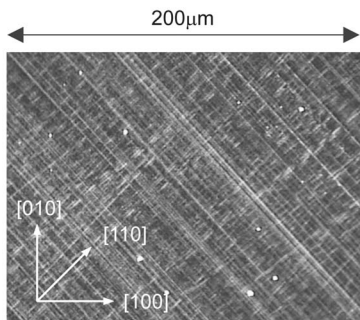
200μm

FIG. 7. Optical microscope image showing the cross-hatch morphology typical of virtual substrates.

As Fe/Ge(001) and Fe/Ge/Si$_{1-x}$Ge$_x$/Si(001) essentially display the same magnetic and structural properties,[7] also in Fe/Ge/Si$_{1-x}$Ge$_x$/Si(001) we can associate the uniaxial anisotropy with easy axis [010] to deposition at oblique incidence and substrate sputtering procedures. The values of $K_u^{[010]}/K_1$, however, even considering an error of 10^{-3} on 15 ML and 5×10^{-4} on 30 and 60 ML (associated to a maximum error on $K_u^{[010]}/M$ of ± 0.05 Oe, and assuming $K_1/M = 50$ Oe for 15 ML and 100 Oe for 30 and 60 ML), show a nonmonotone evolution with a minimum at 30 ML, that we attribute to the superposition of the two anisotropy sources. Sputtering is more efficient in determining the uniaxial anisotropy at low coverages, while the influence of out-from-normal deposition increases with coverage. The combination of these two effects, the first decreasing and the other increasing with film thickness, could well explain our findings, setting 30 ML as a turning point.

C. Discussion: ultrathin films (5–10 ML)

We consider now the low thickness regime. In order to explain the higher uniaxial anisotropy with [110] easy axis evidenced by SPIPE in the case of Fe/Ge/Si$_{1-x}$Ge$_x$/Si(001), we must consider the peculiar morphology of virtual substrates. Figure 7 reports an image of the Ge(1 μm)/Si$_{1-x}$Ge$_x$(10 μm)/Si(001) virtual substrate employed: a cross-hatch pattern is evident, characterized by a rms roughness of 3 nm and a periodicity of roughly 500 nm, due to dislocations formed to relieve the Si-Ge mismatch.[33] The edges are oriented along the [110] and [$\bar{1}$10] directions, so that they may well contribute to the [110] uniaxial anisotropy, in addition to interface effects arising from dangling bonds directionality. It is clearly visible in Fig. 7 that the two directions [110] and [$\bar{1}$10] are not exactly equivalent, however, at present we do not have any explanation of why the [110] direction dominates.

The analysis of MOKE data is more complex in this case as both the $K_u^{[110]}$ and $K_u^{[010]}$ anisotropy terms must be taken into account. Moreover, the simple model developed in Ref. 19 is no more satisfactory, because at low coverages effects arising from coherent rotation are clearly visible in the hysteresis loops. For this reason, in order to fit the data and extract the magnetic parameters, we have applied the numerical code illustrated in Sec. A. The results of this procedure for 10 ML of Fe are reported in Table III, while the

TABLE III. Magnetic parameters of Fe/Ge/Si$_{1-x}$Ge$_x$/Si(001) film with thickness of 10 ML. The accuracies are ±1 Oe on the anisotropy constants and ±0.5 Oe on the energy barriers.

$\dfrac{K_1}{M}$ [Oe]	$\dfrac{K_u^{[010]}}{M}$ [Oe]	$\dfrac{K_u^{[110]}}{M}$ [Oe]	$\dfrac{\varepsilon_{90}}{M}$ [Oe]	$\dfrac{\varepsilon_{180}}{M}$ [Oe]	$\dfrac{K_u^{[010]}}{K_1}$	$\dfrac{K_u^{[110]}}{K_1}$
30	5.5	31	10.3	14.0	18.3%	>1

experimental (empty dots) and the simulated loops (continuous lines) are shown in Fig. 8. The angle between M_0 and [100], when H is applied along the [100] direction, is $\theta_0 = 60.85°$, in agreement with the SPIPE results reported in Fig. 3(b).

The cubic term K_1/M is definitively lower than the bulk value for bcc Fe (275 Oe) but comparable with the lowest value compatible with the 15 ML film (50 Oe), as discussed before. By consequence the ratio $K_u^{[010]}/K_1$ is larger than in thicker films, while the uniaxial anisotropy related to the substrate is comparable with the cubic term.

Finally, longitudinal MOKE data for 5 ML coverage, with H applied along [100], are reported in Fig. 9 (empty circles) along with the best fit (continuous line). A good numerical simulation can be obtained only by setting $K_u^{[010]}=0$ and keeping only the interface uniaxial term $K_u^{[110]}$. This reflects the superposition of the two sources discussed above: the cross-hatch pattern of the virtual substrate and the directionality of dandling bonds. As a result, in 5 ML Fe/Ge/Si$_{1-x}$Ge$_x$/Si(001), the $K_u^{[110]}$ term completely hides the $K_u^{[010]}$ contribution, while in the Fe/Ge(001) film both are present. In principle, the cross hatch is similar to the ripples produced by ion sputtering at oblique incidence, and, since
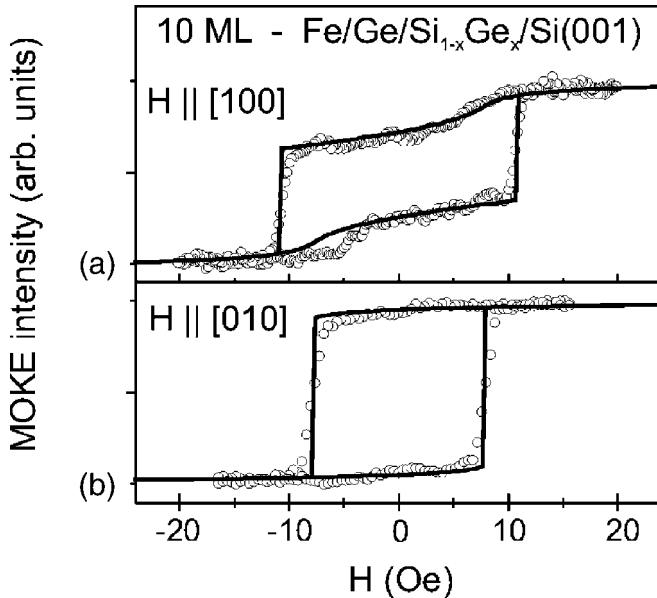

FIG. 8. Measured (empty circles) and simulated (continuous line) hysteresis loops from 10 ML Fe/Ge/Si$_{1-x}$Ge$_x$/Si(001) film: (a) longitudinal loop; (b) transverse loop.
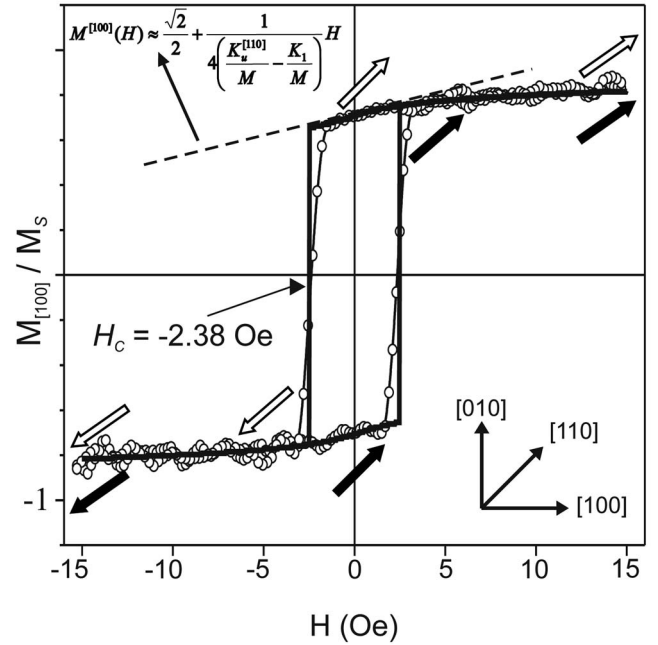

FIG. 9. Measured (empty circles) and simulated (continuous line) longitudinal hysteresis loop on 5 ML Fe/Ge/Si$_{1-x}$Ge$_x$/Si(001) film with the external field H applied along [100]. The direction of M at different values of H is indicated by arrows.

sputtering is done with (010) incidence plane, we could expect a sort of interference. However the cross hatch is characterized by a rms roughness of 3 nm and a periodicity of roughly 500 nm, a much more pronounced morphology than the one possibly produced by sputtering (roughness and periodicity of 1.1 and of ~200 nm, respectively[25]). Moreover the sputtering influence should be considerably reduced by the subsequent annealing procedures, so that its effect can be neglected. On the other hand, the influence of out-from-normal deposition is expected be very small at 5 ML. As a result, the cross-hatch morphology is the dominant source of anisotropy.

We consider now the details of the hysteresis loop of Fig. 9 in order to extract the anisotropy constants. When H decreases from positive to negative values along the [100] direction, a sharp transition occurs at $H_C \approx -2.38$ Oe. In this point M rotates from $\theta \approx 49°$ to $\theta \approx 221°$ as a result of the sum of nucleation and propagation of domains at 180° (associated to an energy barrier of $\varepsilon_{180}/M=3.50$ Oe), and of a coherent clockwise rotation of 8°; the total effective rotation of M is $\Delta\theta=172°$. At $H=0$ the fit predicts $\theta=45°$: M_0 is then oriented along [110], in perfect agreement with SPIPE [cf. Fig. 3(b)].

In order to get K_1 and $K_u^{[110]}$ values without assumptions on K_1, we performed an analytical fitting of the hysteresis loop around $H=0$ (see Appendix), that can be applied in this relatively simple case with only one uniaxial anisotropy. For small external fields the magnetization M normalized to the saturation value can be written as

$$\frac{M_{[100]}(H)}{M_S} \approx \frac{\sqrt{2}}{2} + \frac{1}{4\left(\dfrac{K_u^{[110]}}{M} - \dfrac{K_1}{M}\right)}H. \tag{8}$$

By fitting the experimental data with Eq. (8), the difference $K_u^{[110]}/M - K_1/M$ results 10 ± 1 Oe, so that the ratio $K_u^{[110]}/K_1$ is greater than one, regardless of the effective value of K_1. This is extremely different from the case of $K_u^{[010]}$, whose contribution is lower than 20% of K_1 for all the films investigated.

As a final remark, we note that for possible applications a protecting capping of the Fe/Ge films would be needed; this could well give rise to strong variations of the magnetic anisotropies. Indeed, preliminary measurements on a 60 ML thick Fe film on Ge virtual substrate, capped with 30 Å of Au, show less squared loops with an increase of $K_u^{[010]}/M$ and no change of ε_{90} and ε_{180}. A systematic study of these effects is however, well beyond the purpose of the present paper.

V. CONCLUSIONS

To summarize, Fe films have been grown at room temperature onto virtual Ge/Si$_{1-x}$Ge$_x$/Si(001) and standard single crystal Ge(001) substrates, and their magnetic anisotropies have been extensively investigated by SPIPE and MOKE. In particular, SPIPE has been employed in a unusual way in order to find the direction of the remanent magnetization M_0. This method proves to be efficient, does not require any kind of arbitrary model in order to interpret the results, and is very surface sensitive, compared to classical magneto-optical techniques. MOKE loops, recorded on Fe films on Ge/Si$_{1-x}$Ge$_x$/Si(001) in the thickness range 5–60 ML, were fitted by a phenomenological model. They can be interpreted as the superposition of a cubic (K_1) and two uniaxial anisotropies, with easy axis along [010] ($K_u^{[010]}$) and [110] ($K_u^{[110]}$), respectively. $K_u^{[110]}$ is associated to the Fe/Ge interface: indeed it disappears above 10 ML; in very thin films (5 ML) on virtual substrates it is stronger than the cubic term ($K_u^{[110]}/M - K_1/M = 10$ Oe) and drives the orientation of M_0. On the contrary, $K_u^{[010]}$ is mainly associated with bulk properties. It persists even at large thicknesses (60 ML) but its strength is lower than K_1. It is related to the preparation conditions of the sample, in particular (i) oblique sputtering on Ge substrate before Fe deposition and (ii) oblique deposition of Fe film. In particular, we find that the uniaxial easy axis is always perpendicular to the plane of incidence of the Fe flux, while sputtering essentially produces a negligible effect. Morphology and preparation conditions strictly influence magnetism in Fe/Ge(001) and Fe/Ge/Si$_{1-x}$Ge$_x$/Si(001) films. The knowledge of these mechanisms paves the way to tune magnetic uniaxial anisotropies of Fe films on Ge(001).

APPENDIX

In order to fit the MOKE loop from 5 ML of Fe on Ge/Si$_{1-x}$Ge$_x$/Si(001) around $H = 0$, we used the following analytical treatment. Eq. (1) without the $K_u^{[010]}$ term becomes

$$E = \frac{K_1}{4} \sin^2 2\theta + K_u^{[110]} \sin^2(\theta - \pi/4) - MH \cos(\theta - \phi).$$
(A1)

The conditions for minima are

$$\frac{\partial E}{\partial \theta} = -K_u^{[110]} \cos 2\theta + \frac{K_1}{2} \sin 4\theta + MH \sin(\theta - \phi) = 0,$$
(A2)

$$\frac{\partial^2 E}{\partial \theta^2} = 2K_u^{[110]} \sin 2\theta + 2K_1 \cos 4\theta + MH \cos(\theta - \phi) > 0,$$
(A3)

and the possible orientations of M_0 can be found by putting $H = 0$ in Eq. (A2)

$$\theta_0 = \pi/4, -3/4\pi \text{ if } K_u^{[110]} > K_1,$$
(A4)

$$\theta_0 = \frac{1}{2} \arcsin \frac{K_u^{[110]}}{K_1} \text{ if } K_u^{[110]} \leq K_1.$$
(A5)

The solution for $K_u^{[110]} \leq K_1$ must be excluded, because the associated loop shape would be incompatible with experimental data in Fig. 9. In between the other solutions (A4) SPIPE allows us to chose the right one, that is $\theta_0 = \pi/4$. $\theta(H)$, around the point $H = 0$, can then be approximated by a linear expansion

$$\theta(H) = \frac{\pi}{4} + \chi H,$$
(A6)

where χ is an arbitrary coefficient to be determined. Using Eq. (A6) and setting $\phi = 0$ (H applied along [100]), Eq. (A2) becomes

$$\frac{\partial E}{\partial \theta} = 2K_u^{[110]} \chi H - 2K_1 \chi H + \frac{\sqrt{2}}{2} MH(1 + \chi H) = 0. \quad (A7)$$

Neglecting second-order terms in H^2 and excluding the trivial solution $H = 0$, an expression for χ is found, that can be replaced in Eq. (A6) to give

$$\theta(H) = \frac{\pi}{4} - \frac{\sqrt{2}M}{4(K_u^{[110]} - K_1)} H.$$
(A8)

This solution satisfy Eq. (A3). Finally, the expression for $M_{[100]}/M_S$ around $H = 0$ is

$$\frac{M_{[100]}(H)}{M_S} = \cos[\theta(H)] = \cos\left[\frac{\pi}{4} - \frac{\sqrt{2}M}{4(K_u^{[110]} - K_1)}H\right] \approx \frac{\sqrt{2}}{2} + \frac{1}{4\left(\frac{K_u^{[110]}}{M} - \frac{K_1}{M}\right)}H. \tag{A9}$$

[1] *Ultrathin Magnetic Structures*, edited by J. A. C. Bland and B. Heinrich (Springer, Berlin, 1994), Vols. I and II.

[2] J. M. De Teresa, A. Barthélémy, A. Fert, J. P. Contour, F. Montagne, and P. Seneor, Science **286**, 507 (1999).

[3] R. Moroni, D. Sekiba, F. Buatier de Mongeot, G. Gonella, C. Boragno, L. Mattera, and U. Valbusa, Phys. Rev. Lett. **91**, 167207 (2003).

[4] R. A. Hyman, A. Zangwill, and M. D. Stiles, Phys. Rev. B **58**, 9276 (1998).

[5] R. P. Cowburn, S. J. Gray, and J. A. C. Bland, Phys. Rev. Lett. **79**, 4018 (1997).

[6] M. Cantoni, M. Riva, G. Isella, R. Bertacco, and F. Ciccacci, J. Appl. Phys. **97**, 093906 (2005).

[7] A. Brambilla, L. Duó, M. Cantoni, M. Riva, R. Bertacco, M. Portalupi, and F. Ciccacci, Solid State Commun. **135**, 158 (2005).

[8] "Virtual" substrate is a technical term commonly used for Ge/Si$_{1-x}$Ge$_x$/Si etherostructures: they are not "real" substrates as single-crystal Ge, but they can used for the same aim in order to grow overlayers on high-quality Ge surfaces. See, e.g., S. G. Thomas *et al.*, J. Electron. Mater. **32**, 976 (2003).

[9] P. Ma and P. R. Norton, Phys. Rev. B **56**, 9881 (1997).

[10] S. Tari, R. Sporken, T. Aoki, D. J. Smith, V. Metlushko, K. AbuEl-Rub, and S. Sivananthan, J. Vac. Sci. Technol. B **20**, 1586 (2002).

[11] U. Valbusa, C. Boragno, and F. Buatier de Mongeot, J. Phys.: Condens. Matter **14**, 8153 (2002).

[12] M. Kummer, C. Rosenblad, A. Domman, T. Hackbarth, G. Höck, M. Zeuner, E. Müller, H. von Känel, Mater. Sci. Eng., B **89**, 288 (2002).

[13] R. Bertacco, M. Cantoni, M. Riva, A. Tagliaferri, and F. Ciccacci, Appl. Surf. Sci. **252**, 1754 (2005).

[14] J. M. Florczak and E. Dan Dahlberg, J. Appl. Phys. **67**, 7520 (1990).

[15] M. Cantoni and R. Bertacco, Rev. Sci. Instrum. **75**, 2387 (2004).

[16] In literature, out-of-plane components in Fe/Ge films are generally excluded "*a priori*." In our work, we recorded the intensities associated with the components of the reflection matrix r_{SP} and r_{PS} by MOKE: the result is identical within our experimental accuracy, so that out-of-plane components can be finally ruled out.

[17] J. Kessler, *Polarized Electrons*, in Springer Series on Atoms and Plasmas (Springer, Berlin, 1985).

[18] F. Ciccacci and S. De Rossi, Phys. Rev. B **51**, 11538 (1995).

[19] R. P. Cowburn, S. J. Gray, J. Ferré, J. A. C. Bland, and J. Miltat, J. Appl. Phys. **78**, 7210 (1995).

[20] J. J. Krebs, B. T. Jonker, and G. A. Prinz, J. Appl. Phys. **61**, 2596 (1987).

[21] M. Marangolo, F. Gustavsson, G. M. Guichar, M. Eddrief, J. Varalda, V. H. Etgens, M. Rivoire, F. Gendron, H. Magnan, D. H. Mosca, and J.-M. George, Phys. Rev. B **70**, 134404 (2004).

[22] J. H. Wolfe, R. K. Kawakami, W. L. Ling, Z. Q. Qiu, R. Arias, and D. L. Mills, J. Magn. Magn. Mater. **232**, 36 (2001).

[23] Y. Park, E. E. Fullerton, and S. D. Bader, Appl. Phys. Lett. **66**, 2140 (1995).

[24] S. van Dijken, G. Di Santo, and B. Poelsema, Phys. Rev. B **63**, 104431 (2001).

[25] E. Chason, T. M. Mayer, B. K. Kellerman, D. T. McIlroy, and A. J. Howard, Phys. Rev. Lett. **72**, 3040 (1994).

[26] Y. Z. Wu, C. Won, and Z. Q. Qiu, Phys. Rev. B **65**, 184419 (2002).

[27] H. C. Mireles and J. L. Erskine, Phys. Rev. Lett. **87**, 037201 (2001).

[28] G. Bertotti, in *Hysteresis in Magnetism* (Academic Press, New York 1998).

[29] H. P. Oepen, C. M. Schneider, D. S. Chuang, C. A. Ballentine, and R. C. O'Handley, J. Appl. Phys. **73**, 6186 (1993).

[30] M. Brockmann, M. Zölfl, S. Miethaner, and G. Bayreuther, J. Magn. Magn. Mater. **198**, 384 (1999).

[31] M. Cantoni, M. Riva, G. Isella, R. Bertacco, and F. Ciccacci, Appl. Surf. Sci. **252**, 5304 (2006).

[32] Note that this analysis applies to thick films on single crystal substrates as well.

[33] P. M. Mooney, J. L. Jordan-Sweet, I. C. Noyan, S. K. Kaldor, and P.-C. Wang, Appl. Phys. Lett. **74**, 726 (1999).